Food Texture Measurement System Using Rod Type Actuator for Imitation of Human Mastication

Nakamoto, Hiroyuki
Nagahata, Yuya
Kobayashi, Futoshi

(Citation)
International Journal of Automation Technology,16(4):421-426

(Issue Date)
2022-07-05

(Resource Type)
journal article

(Version)
Version of Record

https://doi.org/10.20965/ijat.2022.p0421

Technical Paper:

Food Texture Measurement System Using Rod Type Actuator for Imitation of Human Mastication

Hiroyuki Nakamoto*,†, Yuya Nagahata, and Futoshi Kobayashi***

*Kobe University
1-1 Rokkodai-cho, Nada-ku, Kobe, Hyogo 657-8501, Japan
†Corresponding author, E-mail: nakamoto@panda.kobe-u.ac.jp
**J-Oil Mills, Inc., Tokyo, Japan

[Received November 8, 2021; accepted January 5, 2022]

Food texture is one of the most important factors in determining the personal palatability of foods, so food companies require food texture measurement and evaluation in developing novel food products. However, instruments are not fast enough or strong enough to imitate human mastication. To measure the textures of different foods, this study proposes a sensor stand that uses a rod-type actuator. The target speed and force of the sensor stand are 100 mm/s and 100 N, respectively. A food texture sensor that imitates the structure of a human tooth is attached to the sensor stand. The sensor stand and a desktop computer make up the measurement system. Using the system, the fundamental characteristics of the sensor stand with the texture sensor are demonstrated. Verification experiments confirm that the sensor stand satisfies the target values of speed and force. Experiments on actual food items also demonstrate the effectiveness of the measurement system in evaluating food textures.

Keywords: food texture, texture measurement, rod-type actuator, mastication, food evaluation

1. Introduction

When people chew their food, they perceive its taste, aroma, and texture, and these enable them to recognize the flavor and palatability of what they are eating. This makes the measurement and evaluation of taste, aroma, and texture important in food development. To measure taste components, Toko developed a method for measuring taste [1, 2]. The instrument that uses this method is commercially available and has been used by food developers the world over [3]. Regarding aroma, some devices that measure it have been reported [4, 5]. On the other hand, the palatability of foods is determined mostly by texture [6, 7], and texture actually contributes more to taste than does aroma. To add texture to food, some devices that provide a user with a food texture have been reported [8, 9]. These trials are interesting, but since consumers generally prefer to eat foods with pleasant textures, texture is a significant factor in determining the sales of food items. Food companies need ways of measuring and evaluating food textures.

In food texture measurement, major instruments consist of a load cell and a motorized slider. The motorized slider imitates the motion of chewing. The instruments use a probe to measure the time-series force or pressure in two compressions of the food. The texture profile analysis (TPA) determines the physical properties from the measurement data [10, 11]. Although the TPA is effective in the evaluation of texture, the characteristics of the instruments are different from those of the motion of human mastication. One of the different characteristics is speed. Humans chew hard foods slowly and soft foods relatively quickly. In fast chewing, the speed rises to 74 mm/s [12]. On the other hand, the compression speed of the instruments is 10–20 mm/s. Due to the low speed, the instruments cannot recreate the motion of human mastication. Kinumatsu et al. have developed an instrument that moves the probe at the speed of 100 mm/s [13]. Akimoto et al. have proposed a measurement device using a free-running probe and Sakurai et al. have developed a swing-arm measurement device [14, 15]. Although these devices were capable of raising the speed to 100 mm/s, they did not use the measurement data in the high-speed compression for texture evaluation. When foods were viscous, the reflected force to compression depended on the speed of the probe. In addition to the speed, the measurement of hard foods such as carrots and rice crackers requires sufficient compression force. Depending on the size of the sample, a force of 100 N may be required to compress the food [11]. Shimada et al. measured the dynamic bite force of the molar teeth during mastication and the force was within 100 N [16]. The measurement and evaluation of texture require the same compression speed and force as those of human mastication.

This study proposes a device that imitates the motion of human mastication. We design and produce a moving device that uses a rod-type actuator as a sensor stand. The target speed and force of the sensor stand are 100 mm/s and 100 N, respectively. We have also developed a food texture sensor that imitates the structure of the human tooth and periodontal membrane [17, 18]. The texture sensor has a range of over 100 N and a sampling frequency of 10 kHz, so the sensor stand is suitable for the

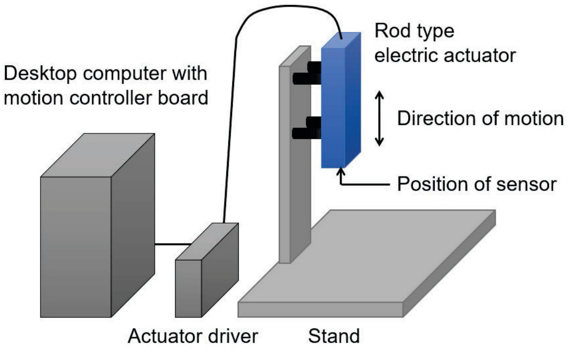

Fig. 1. Structure and components of sensor stand.

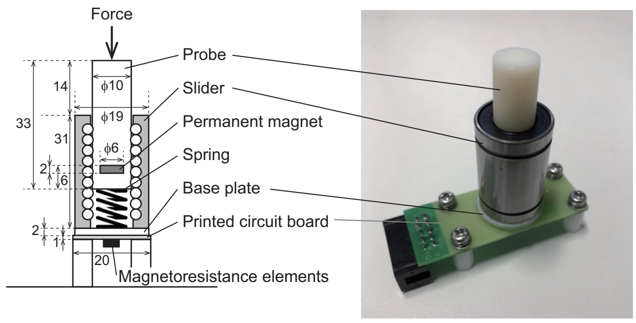

Fig. 2. Structure of texture sensor and its prototype.

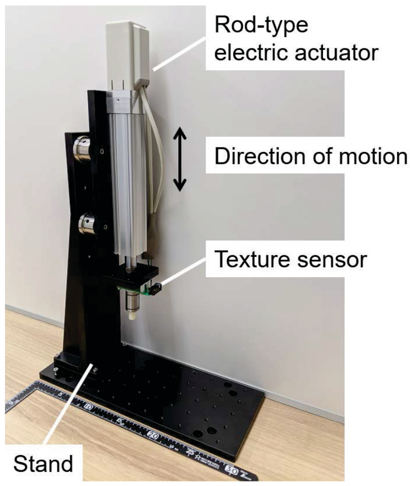

Fig. 3. Sensor stand with rod-shaped electric actuator and texture sensor.

characteristics of the texture sensor. In the following sections, the structure and components of the sensor stand and texture sensor are explained. A measurement system is also included. The fundamental characteristics of the sensor stand with the texture sensor are revealed through experiments using the measurement system. Finally, the effectiveness of the sensor stand is discussed.

2. Measurement System Using a Rod-Type Electric Actuator

2.1. Sensor Stand with Rod-Type Electric Actuator

The structure of the sensor stand is shown in **Fig. 1**. The sensor stand consists of an actuator, an actuator driver, a desktop computer with a motion controller board, and a stand. The actuator is a rod-type electric actuator having a step motor (LEY16D, SMC Co., Tokyo, Japan) [19]. Two electric actuators are used according to the application. One is used for high-speed motion over 100 mm/s; the other is used for high force motion over 100 N. The difference between them is the lead length of the screw shaft. The lead lengths of the former and latter are 10 and 2.5 mm, respectively. The actuators can be mounted to the stand quickly. They have a 100-mm stroke and a positioning repeatability of ±0.02 mm. A motion controller (SMC-4DL-PE, Contec Co., Ltd., Osaka, Japan) which is embedded into a desktop computer drives the actuators via an actuator driver (LECPA, SMC Co., Tokyo, Japan). The motion controller and the actuator driver are common devices for the two actuators.

2.2. Food Texture Sensor

The food texture sensor consists mainly of a probe, a linear slider, a spring, and a circuit board [18]. **Fig. 2** is a schematic drawing and a photo of the sensor structure. The probe is a cylindrical shape with a 10 mm diameter. It was made by a 3D printer from acrylonitrile-butadiene-styrene resin, but it has a cylindrical magnet within it. There is a spring at the bottom of the probe, and the ends of the spring are fixed to the probe and the base plate. The spring determines the vertical position of the probe based on an external force to the probe. The linear slider limits the motion of the spring to the vertical direction. The circuit board has two magnetoresistive elements and is connected to an amplifier circuit which amplifies their output voltages 59.4 times. The amplifier circuit is connected to the desktop computer via an A/D conversion board. The A/D conversion board converts the amplified voltages to 16-bit digital data with the sampling frequency of 10 kHz and sends the data to the computer. The computer calculates the acting force F on the sensor's probe from the voltages of the magnetoresistive element by using the following calibration equation.

$$F = c_0 + \frac{c_1}{v_1} + \frac{c_2}{v_1^2} + \frac{c_3}{v_2} + \frac{c_4}{v_2^2} \quad \text{. . . . . (1)}$$

where c_i $(i = 0, \ldots, 4)$ are coefficients determined by a calibration, and v_1 and v_2 are the amplified voltage of the magnetoresistive elements.

2.3. Measurement System

The sensor stand with the food texture sensor is shown in **Fig. 3**. The height of the top of the actuator is 460 mm; the area of the base plate of the stand is 120×300 mm. The computer controls the actuator and obtains measurement data from the food texture sensor. Although the

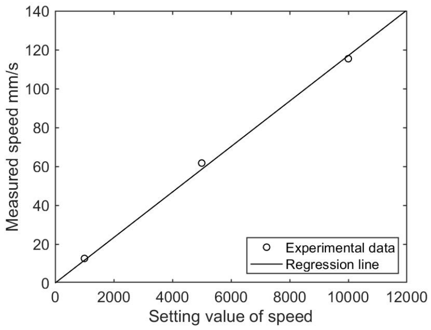

Fig. 4. Relationship between setting speed and experimental speed.

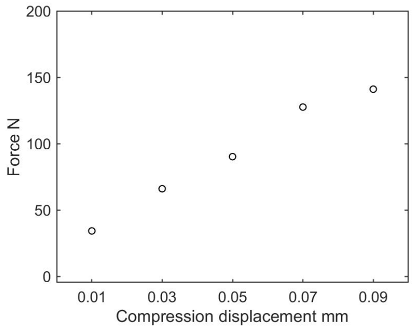

Fig. 5. Relationship between displacement and force in the cumulatively increasing compression displacement.

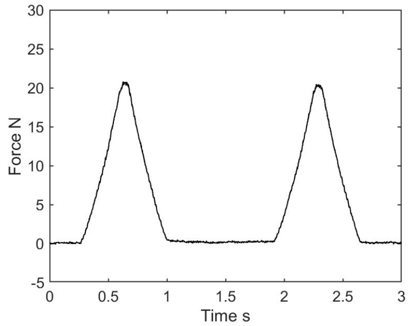

Fig. 6. Relationship between time and force in two compressions.

procedure of the control and the measurement depends on the physical properties of the target food, for a snack food such as a french fry, the food texture sensor compresses the snack to the compression rate of 80% or 90%. In this case, the food texture sensor measures the heights of the top and bottom surfaces of the food by contact and the computer determines the stroke length of the actuator based on the thickness of the food as calculated from the initial heights. After that, the computer compresses the food twice, based on the stroke length and the set speed. Some parameters such as hardness and springiness are calculated from the measured force data attained through the TPA analysis. For crisp and brittle foods, such as crackers or potato chips, a single compression is used, and the hardness is calculated from the peak of the measured force data.

3. Experiment

3.1. Speed and Compression Force of Sensor Stand

The target speed of the movement of the sensor stand was over 100 mm/s. First, a fundamental experiment verified that the sensor stand satisfied the target speed. In this experiment, a laser distance sensor was put on the base plate of the stand and the displacement of the tip of the probe on the texture sensor was measured. The computer set three speeds for the motion controller, 1000, 5000, and 10000, and it made the movement of the tip of the probe 50 mm. The speed was calculated from the time interval and the measured displacement of the movement. The relationship between the set speed and the test speed is shown in **Fig. 4**. The line represents the regression line of the test data. The relation was linear and the coefficient of determination was 0.99.

Second, to confirm the compression force of the sensor stand, we performed the following experiment. A force sensor (MINI 8/40-A, BL Autotec, Ltd., Kobe, Japan) was attached to the sensor stand. The force sensor had a stainless steel probe with a cylindrical shape 10-mm in diameter and a measurement range of over 150 N. In the experiment, the probe touched a wooden block. After a preparatory press with a displacement length of 0.01 mm, the sensor stand cumulatively compressed the block four times with a displacement length of 0.02 mm. The relationship between displacement and force is shown in **Fig. 5**. The force after three and four compressions was over 100 N.

3.2. Fundamental Experiment Using Measurement System

The measurement system, in which the sensor stand had the food texture sensor on the tip of the actuator, compressed a urethane sheet. The urethane sheet was 5 mm in thickness and had an Ascar-C hardness of 30. The spring constant of the spring in the sensor was 5.9 N/mm. The measurement system compressed the urethane sheet two times with the sensor at a speed of 10 mm/s and a stroke length of 6.0 mm. The initial gap between the probe surface of the sensor and the sheet was about 2.5 mm. The relationship between time and the force measured by the sensor is shown in **Fig. 6**. The peaks were approximately 20 N and the wave shapes were nearly identical. The measurement system compressed a urethane sheet one time at six different speeds: 10, 20, 30, 40, 50, and 60 mm/s. The other conditions were the same in the above experiment. The measured forces with the different speeds are shown in **Fig. 7**. The faster the speed, the sharper the shape of the force data. The peak of force increased as the speed increased because the viscosity of the urethane sheet increased the reaction force.

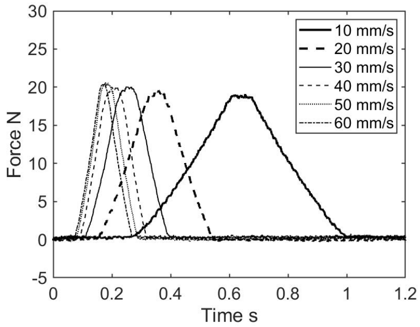

Fig. 7. Relationship between time and force at six different speeds.

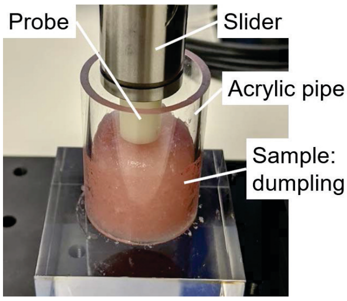

Fig. 8. Probe and slider of food texture sensor testing sample in acrylic resin tube.

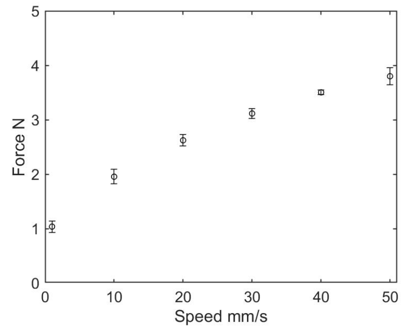

Fig. 9. Relationship between compression speed and measured maximum force. The marker and error bar show the mean and range of standard deviation of 10 measurements, respectively.

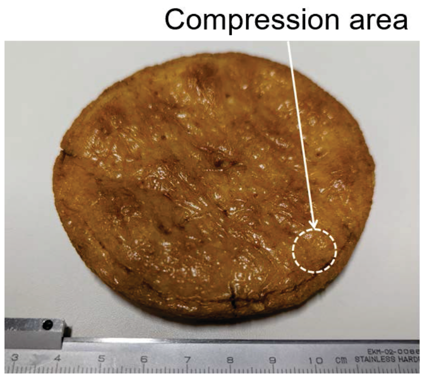

Fig. 10. Rice cracker sample.

3.3. Measurement Example of Viscoelastic Food

Many foods have both elastic and viscous characteristics. The measurement system gives a food sample a stroke-constant compression. In this case, one of the simple physical models of food is the Voigt model. The Voigt model consists of the sum of an elastic term and a viscous term as the following equation using stress p and strain ε.

$$p = E\varepsilon + \eta \frac{d\varepsilon}{dt}, \quad \quad (2)$$

where E is a modulus of elasticity and η is a viscosity. If the stroke length, i.e., strain, in the measurement is constant, the elasticity term is also constant. On the other hand, the viscosity term depends on the speed of the compression strain. By using the variety of the compression speed, the measurement system with the food texture sensor obtained the differences in the viscosity term.

An experiment to verify the differences in the viscous term was performed as follows. The food sample was a sweet rice dumpling (Kushi-dango, Consumers Co-operative Kobe, Kobe, Japan). Because of the repetitive compressions, the sample was put into an acrylic resin tube 30 mm in diameter, 2 mm in thickness, and 60 mm in length as shown in **Fig. 8**. The sample was pink in color. Because the deformation remained after compression, we made the surface of the sample flat. The length of compression was constant at 5 mm. The compression speeds were 1, 10, 20, 30, 40, and 50 mm/s. The relationships between the speed of compression and the force are shown in **Fig. 9**. Although the increment of the force to the speed was not linear, the force increased as the speed increased.

3.4. Example Measurement of Hard Food

To confirm the effectiveness of the high force of the sensor stand, the measurement system measured a rice cracker as an example of hard food. The rice cracker (Atsuyaki, Kingodo, Co., Tokyo, Japan) is shown in **Fig. 10**. It was about 80 mm in diameter and about 9 mm in thickness. The texture sensor compressed the area indicated by the dashed line by a length of 7 mm from the point of the contact position and at a speed of 10 mm/s. The relationship between time and force is shown in **Fig. 11**. The compression force rapidly rose to about 55 N and the rice cracker broke at about 0.5 s. After that, the texture sensor compressed the fragments of the rice cracker and detached them at about 0.7 s.

4. Discussion

The rod-type electric actuator using a step motor was mounted on the sensor stand. Based on human mastication, the target speed and force were 100 mm/s and 100 N, respectively. After the measurement system was readied,

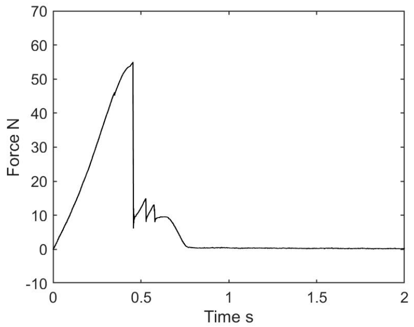

Fig. 11. Relationship between time and force in compression of rice cracker.

the performances of the sensor stand and the system were verified.

The speed and force of compression were tested first. **Fig. 4** shows that the relationship between the setting and measured speeds was linear and that they had a high determination coefficient. The maximum speed was over 100 mm/s. The measurement system can set the speed by using the linear relationship. **Fig. 5** shows that the sensor stand with the force sensor compressed the wooden block at a force of over 100 N. **Fig. 5** also indicates the linear relationship between the displacement of 10 μm and the force. Hence, the sensor stand satisfied the target values of speed and force.

The measurement system measured the reflected force from the urethane sheet in the two compressions. The two wave shapes and peaks in **Fig. 6** correspond. This two-compression measurement was frequently used in the TPA. The result revealed that the sensor stand was capable of stable movement. The higher speeds made the sharper slopes seen in **Fig. 7**. The starting times of slope of 10, 20, 30, 40, 50, and 60 mm/s were 0.27, 0.14, 0.11, 0.09, 0.08, and 0.07 s, respectively. Although the starting times should be proportional to the speed, the relation was not proportional because the actuator required time to accelerate to the set speed. In general, if the sensor stand attains a higher speed, the initial distance between the tip of the sensor probe and the sample should be properly determined based on the acceleration time. In **Fig. 7**, the waves of 50 and 60 mm/s have almost the same shape. After the sensor probe touches a sample, the force from the sample is reflected to the actuator, and its speed decreases. For measurements, the most suitable speed of compression should be confirmed in advance.

Figure 9 shows the effects of speed in the experiment carried out on the rice dumpling. The relationship of the incrementation of the force to the speed was not linear. This did not coincide with the Voigt model. Because the Voigt model has two elements of elastic and viscous terms and is simple in structure, it might not be sufficiently accurate to express the characteristics of the dumpling. To identify the structure as a multi-element model, an analysis using the additional data of the different speeds and the creep curves is required. The sensor stand can provide further analysis with measurement data.

The system also obtained measurement data on the rice cracker which is a comparatively hard food. **Fig. 11** shows the first fracture at over 50 N and the other two small fractures. The first slope was almost constant. **Fig. 5** shows that the sensor stand is capable of a compression force of over 100 N, so it clearly has enough force to compress and fracture comparatively hard foods.

5. Conclusions

This paper has proposed a motion device with a rod-type actuator. The target speed and force of the sensor stand are 100 mm/s and 100 N, respectively. Test data has proven that the sensor stand satisfies the target values. A measurement system combining the sensor stand and a texture sensor has also been developed. Through experiments using a rice dumpling and a rice cracker, the sensor stand and texture sensor have been proven effective in the measurement of the viscoelastic characteristics of food and in the measurement of the hardness of crisp food.

In the future, the measurement system will be used to measure and evaluate the textures of various other foods.

Acknowledgments

This research is partly supported by Adaptable and Seamless Technology transfer Program through Target-driven R&D (A-STEP) from Japan Science and Technology Agency (JST) and JSPS KAKENHI Grant Number JP20K12026.

References:

[1] K. Toko, "A taste sensor," Meas. Sci. and Technol., Vol.9, No.12, pp. 1919-1936, doi: 10.1088/0957-0233/9/12/001, 1998.

[2] K. Toko, "Taste sensor," Sens. and Actuators B: Chem., Vol.64, No.1, pp. 205-215, doi: 10.1016/S0925-4005(99)00508-0, 2000.

[3] Intelligent Sensor Technology, Inc., "What is a Taste Sensor?." http://www.insent.co.jp/en/products/taste_sensor_index.html [Accessed November 1, 2021]

[4] P. Dani and T. Nakamoto, "Sensory Evaluation of Odor Approximation Using NMF with Kullback-Leibler Divergence and Itakura-Saito Divergence in Mass Spectrum Space," J. of The Electrochem. Soc., Vol.167, No.16, 167520, doi: 10.1149/1945-7111/abd110, 2020.

[5] R. Yatabe, A. Shunori, B. Wyszynski, Y. Hanai, A. Nakao, M. Nakatani, A. Oki, H. Oka, T. Washio, and K. Toko, "Odor Sensor System Using Chemosensitive Resistor Array and Machine Learning," IEEE Sens. J., Vol.21, No.2, pp. 2077-2083, doi: 10.1109/JSEN.2020.3016678, 2021.

[6] K. Nishinari, "Rheology, Food Texture and Mastication," J. of Texture Stud., Vol.35, No.2, pp. 113-124, doi: 10.1111/j.1745-4603.2004.tb00828.x, 2004.

[7] N. Matsumoto and A. Matsumoto, "Taste of Food," J. of Cookery Sci. of Japan, Vol.10, No.2, pp. 97-101, doi: 10.11402/cookeryscience1968.10.2_97, 1977 (in Japanese).

[8] H. Tanaka, N. Koizumi, U. Uema, and M. Inami, "Chewing Jockey: Augmented Food Texture by Using Sound Based on the Cross-Modal Effect," SIGGRAPH Asia 2011 Emerg. Technol., 18, 2011.

[9] H. Endo, H. Kaneko, S. Ino, and W. Fujisaki, "An Attempt to Improve Food/Sound Congruity Using an Electromyogram Pseudo-Chewing Sound Presentation System," J. Adv. Comput. Intell. Intell. Inform., Vol.21, No.2, pp. 342-349, doi: 10.20965/jaciii.2017.p0342, 2017.

[10] A. S. Szczesniak, "Classification of Textural Characteristics," J. of Food Sci., Vol.28, No.4, pp. 385-389, doi: 10.1111/j.1365-2621.1963.tb00215.x, 1963.

[11] M. C. Bourne, "Chapter 4 – Principles of Objective Texture Measurement," M. C. Bourne, "Food Texture and Viscosity: Concept and Measurement (2nd Edition)," pp. 107-188, Academic Press, 2002.

[12] T. Takeshita and F. Nakazawa, "Mastication Velocity of the First Molar in Relation to the Mechanical Properties of Food," J. of Home Econ. of Japan, Vol.58, No.3, pp. 129-137, doi: 10.11428/jhej.58.129, 2007 (in Japanese).

[13] Y. Kinumatsu, Y. Michiwaki, M. Yokoyama, K. Michi, T. Takahashi, and H. Ogoshi, "Food Grouping Based on Human Mastication," J. of the Jpn. Stomatol. Soc., Vol.51, No.1, pp. 35-42, doi: 10.11277/stomatology1952.51.35, 2002 (in Japanese).

[14] H. Akimoto, N. Sakurai, and D. Shirai, "A new device for acoustic measurement of food texture using free running probe," J. of Food Eng., Vol.215, pp. 156-160, doi: 10.1016/j.jfoodeng.2017.07.030, 2017.

[15] N. Sakurai, H. Akimoto, and T. Takashima, "Measurement of vertical and horizontal vibrations of a probe for acoustic evaluation of food texture," J. of Texture Stud., Vol.52, No.1, pp. 25-35, doi: 10.1111/jtxs.12559, 2021.

[16] A. Shimada, Y. Yamabe, T. Torisu, L. Baad-Hansen, H. Murata, and P. Svensson, "Measurement of dynamic bite force during mastication," J. of Oral Rehabil., Vol.39, No.5, pp. 349-356, doi: 10.1111/j.1365-2842.2011.02278.x, 2012.

[17] H. Nakamoto, D. Nishikubo, and F. Kobayashi, "Food texture evaluation using logistic regression model and magnetic food texture sensor," J. of Food Eng., Vol.222, pp. 20-28, doi: 10.1016/j.jfoodeng.2017.11.008, 2018.

[18] K. Kusumi, H. Nakamoto, F. Kobayashi, and Y. Nagahata, "Development of Magnetic Food Texture Sensor with Spring and Sliding Mechanism," 2020 IEEE Sens., pp. 1-4, doi: 10.1109/SENSORS47125.2020.9278861, 2020.

[19] SMC Corporation, Rod Type/Guide Rod Type in WEB Catalog. https://www.smcworld.com/products/en/electric/ [Accessed December 20, 2021]

Name:
Hiroyuki Nakamoto

Affiliation:
Associate Professor, Department of Systems Science, Graduate School of System Informatics, Kobe University

Address:
1-1 Rokkodai-cho, Nada-ku, Kobe, Hyogo 657-8501, Japan

Brief Biographical History:
1999- Researcher, Hyogo Prefectural Institute of Technology
2011- Assistant Professor, Kobe University
2016- Associate Professor, Kobe University

Main Works:
• H. Nakamoto, T. Yasuda, F. Kobayashi, Y. Nagahata, R. Shimizu, and K. Kimura, "Sum of variance for quantifying the variation of multiple sequential data for the crispness evaluation of chicken nugget," J. of Texture Studies, Vol.52, No.4, pp. 470-479, 2021.
• H. Nakamoto, Y. Katsuno, A. Yamamoto, K. Umehara, Y. Bessho, F. Kobayashi, and A. Ishikawa, "Wearable Band-shaped Device and Detection Algorithm for Laryngeal Elevation in Mendelsohn Maneuver," IEEE Sensors J., Vol.21, No.13, pp. 14352-14359, 2021.
• H. Nakamoto, P. Guy, and T. Takagi, "Corrosion Induced Roughness Characterization by Ultrasonic Attenuation Measurement," E-J. of Advanced Maintenance, Vol.11, No.4, pp. 139-146, 2020.

Membership in Academic Societies:
• Institute of Electrical and Electronics Engineers (IEEE)
• Society of Instrument and Control Engineers (SICE)
• Robotics Society of Japan (RSJ)

Name:
Yuya Nagahata

Affiliation:
J-Oil Mills Inc.

Address:
8-11 Akachi-cho, Chuo-ku, Tokyo 104-0044, Japan

Brief Biographical History:
2008- J-Oil Mills Inc.

Main Works:
• "The Formation of Resistant Starch during Acid Hydrolysis of High-amylose Corn Starch," J. of Applied Glycoscience, Vol.60, No.2, pp. 123-130, 2013.

Name:
Futoshi Kobayashi

Affiliation:
Associate Professor, Department of Systems Science, Graduate School of System Informatics, Kobe University

Address:
1-1 Rokkodai-cho, Nada-ku, Kobe, Hyogo 657-8501, Japan

Brief Biographical History:
1999- Research Associate, Nagoya University
2000- Research Associate, Kobe University
2005- Associate Professor, Kobe University

Main Works:
• F. Kobayashi, K. Hasegawa, H. Nakamoto, and F. Kojima, "Motion capture with inertial measurement units for hand/arm robot teleoperation," Int. J. of Applied Electromagnetics and Mechanics, Vol.45, Nos.1-4, pp. 931-937, 2014.
• K. Shimizu, F. Kobayashi, H. Nakamoto, and F. Kojima, "POD Evaluation for Joint Angles from Inertial and Optical Motion Capturing System," E-J. of Advanced Maintenance, Vol.7, No.4, pp. 206-215, 2016.
• F. Kobayashi, Y. Kakizaki, H. Nakamoto, and F. Kojima, "Visualization of Remote Taskspace for Hand/Arm Robot Teleoperation," N. Kubota, K. Kiguchi, H. Liu, and T. Obo (Eds.), "Intelligent Robotics and Applications. ICIRA 2016. Lecture Notes in Computer Science," Vol.9835, pp. 479-487, 2016.
• R. Sakata, F. Kobayashi, and H. Nakamoto, "Body Parts Estimation for Motion Capture System Using Multiple Depth Sensors," Proc. of the 2018 Int. Symp. on Micro-NanoMechatronics and Human Science, pp. 1-5, 2018.

Membership in Academic Societies:
• Institute of Electrical and Electronics Engineers (IEEE)
• Japan Society of Mechanical Engineers (JSME)
• Society of Instrument and Control Engineers (SICE)